Article

Limitations of Photonic Analogue to Digital Conversion Based on Passive Chirp of Ultra-Short Laser Pulses in Optical Fiber

Rostislav Starikov, Evgenii Zlokazov and Vsevolod Nebavskiy *,

Department of Laser Physics, National research nuclear university "MEPhI", Kashirskoe shosse, 31, Moscow, Russian Federation; EYZlokazov@mephi.ru; VANebavskii@mephi.ru; RSStarikov@mephi.ru

* Correspondence: VANebavskii@mephi.ru

Abstract: Application of pulsed optical sources on the base of stable mode-locked lasers, which are known for their very low time jitter, provides the opportunity for creation a high precision photonic analogue to digital converters of signals in the microwave range. However, the repetition rate of modern commercially available mode-locked lasers is limited to a few gigahertz. The increase of repetition rate is possible using the schemes that implement a passive chirp of ultra-short pulses prior to electro-optic amplitude modulator, which is driven by the signal under test, and demultiplexing of modulated signal after a modulator. In the given article we analyzed a continuous time-stretch chirp using single mode fiber as dispersive element. The limitations of input signal bandwidth and source pulses energy are considered.

Keywords: analog-to-digital converter; ENOB; photonic time-stretch; optical sampling; photonic sampling; photonic ADC

1. Introduction

High-precision analogue to digital conversion of microwave signals is a topical problem in the field of radar vision and communication technologies. Photonic analogue to digital converters (PhADC) are perspective when frequency and bandwidth of microwave signals to be measured exceeds from several to tens or even thousands of gigahertz [1–6]. Most of the promising PhADC architectures is optically sampled and electronically quantized PhADC schematically illustrated on Fig.1. The main component of this architecture is a stable pulsed light source, which is used as oscillator for generating a sampling signal. The characteristics of light source, such as repetition rate, pulses temporal width, amplitude noise, phase noise or jitter determine the performance capability of PhADC. Pulsed light sources such as femtosecond mode-locked lasers (MLL) can be used for generation of highly stable microwave signals with jitter value at the attosecond region [7–9]. Electro-optic modulator (EOM) being driven by signal to be digitized modulates the amplitude of a pulses train. Photodetector (PD) transforms optically sampled signal into electronic domain where electronic quantizer (EQ) performs processing of each pulse and assign a digital values to measured signal points. The main problem of the scheme from Fig.1 is the limited repetition pulse rate f_{rep} of commercially available off-the-shelve MLL models, which typically 1.25–2.5 GHz [10], this limits the Nyquist bandwidth of input signal to $f_{rep}/2$.

Using the methods of femtosecond light pulses chirp together with DWDM technology it is possible to increase the sampling rate of PhADC. Fig.2 represents the principal scheme of multichannel optically sampling electronically quantizing PhADC based on passive chirp of femtosecond pulses train. Mode-locked laser emits light pulses with the repetition rate of $f_{rep} = 1/T_{rep}$ where T_{rep} is the period between pulses. Spectral width of subpicosecond gigahertz pulsed laser sources in telecommunication C or L regions is typically above 10 nm that covers up to 12 ITU (100 GHz) channels of a standard telecommunication DWDM module. Module PC performs the passive chirp of light pulses such that selected DWDM

Preprints (www.preprints.org) | NOT PEER-REVIEWED | Posted: 14 November 2022 doi:10.20944/preprints202211.0229.v1

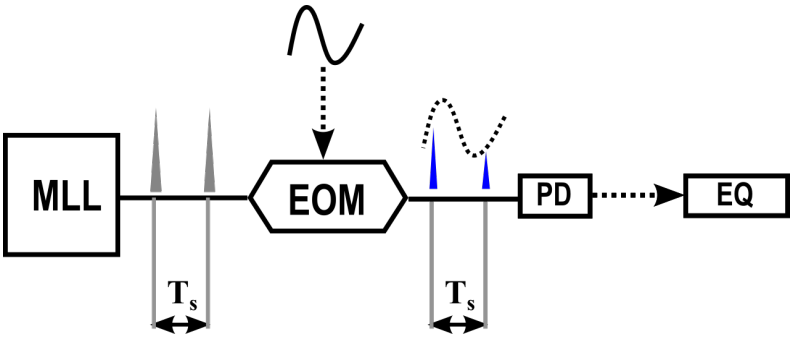

Figure 1. Single channel PhADC scheme: MLL — mode-locked laser; EOM — electrooptic modulator; PD — photo-diode; EQ — electronic quantizer.

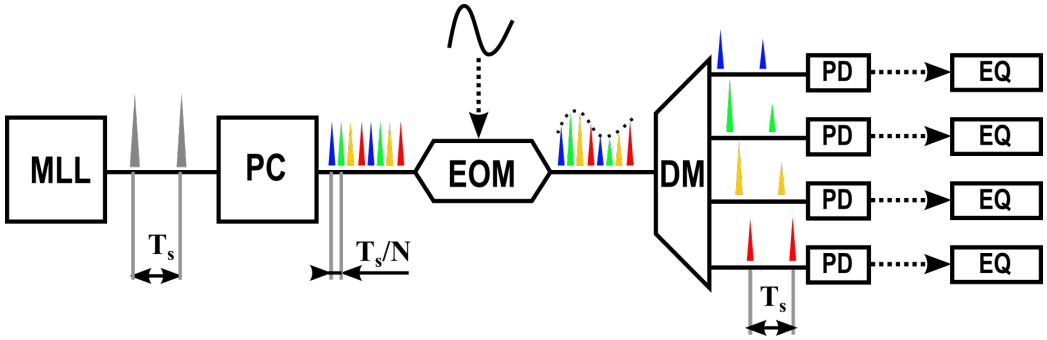

Figure 2. Multichannel PhADC scheme

spectral components are being delayed and placed equidistantly within the repetition period in the output signal. EOM modulates amplitude of chirped pulses train. The combination of PC and EOM performs the time-to-wavelength mapping procedure [3]. Then modulated chirped signal is demultiplexed by (DM), which has PD and EQ on each of the selected channels. The number of the selected DWDM channels N determines the sampling rate of a system, which is $f_s = Nf_{rep}$.

The basic advantage of this approach is the possibility to use "slow" high resolution electronic ADCs in each of the output DWDM channels.

There are numerous methods were proposed to perform the passive chirp of ultra short laser pulses. One of the early approaches use free space optical schemes based on diffraction gratings [11,12] or prisms [13]. These methods were successive for generation of high energy ultra-short pulses however high sensitivity to vibrations and misalignment makes them incompatible for PhADC. Discrete chirp method based on demultiplexer and multiplexer with time delay management in corresponding spectral channels is promising for application in multichannel PhADC scheme [3,14,15]. However, such an architecture is unstable by means of sampling signal phase noise in conditions of high range of outer temperature variation that causes the rise of time delay error between channels due to thermal stretch of fibers. One of the possible ways of discrete chirp practical implementation in PhADC scheme is photonic integrated circuits technologies however it is still under development.

One of the simplest methods to perform the passive chirp of ultra-short light pulses is the use of dispersive elements such as optical fibers. High linearity of second order dispersion effect provides a high stability of time-to-wavelength mapping [16,17].

Significant limitation of ultra-short light pulses chirp using fiber in multichannel PhADC scheme is a fiber length that is required to perform the desired equidistant time shift of selected spectral components. Typically it is in the range of 1–10 km for standard SMF. This problem causes a temporal stretch of spectral components, elongation of sampling gate and consequently limitation of PhADC input bandwidth. Also the non-linear effects such as self-phase modulation becomes valuable since the energy of femtosecond pulses

Preprints (www.preprints.org) | NOT PEER-REVIEWED | Posted: 14 November 2022 doi:10.20944/preprints202211.0229.v1

is being increased above a few picajoules, which deforms the spectrum of a source light pulses train.

In the present article we analyzed a time-to wavelength mapping method using ultra short light pulses chirp in long optical fiber line. The main goal of the research is estimation of input signal bandwidth and maximum source pulses energy limitations.

2. Bandwidth limitation of dispersive chirp PhADC

For ideal ADC the instantaneous values of input Nyquist limited signal are required for lossless reconstruction of a signal from an acquired samples. In the real cases finite aperture of sampling signal limits the bandwidth of input signal.

Consider the sampling process of input microwave signal $x(t)$ by mixing it with sampling signal $p_s(t)$, which mathematically can be described via a pulse envelop function $\phi(t)$ as

$$p_s(t) = \sum_n \phi(t - nT_s), \tag{1}$$

where T_s is sampling period. Periodicity of sampling signal allows to represent if as Fourier series expansion:

$$p_s(t) = \sum_k p_k \exp \frac{j2\pi kt}{T_s}, \tag{2}$$

where

$$p_k = \frac{1}{T_s} \int \phi(t) \exp -\frac{j2\pi kt}{T_s} dt = \frac{1}{T_s} \Phi\left(\frac{k}{T_s}\right) \tag{3}$$

are Fourier coefficients and

$$\Phi(f) = \int \phi(t) e^{-j2\pi tf} dt \tag{4}$$

is sampling pulse envelop function Fourier transformation.

According to Eqs.2–4 spectrum of sampled signal at the output of mixer can be expressed using Fourier transformation as

$$\mathfrak{F}\left[x(t)p_s(t)\right](f) = \frac{1}{T_s} \sum \Phi(kf_s) X(f - kf_s), \tag{5}$$

where f — are Fourier frequencies, $f_s = T_S^{-1}$ is sampling frequency and

$$X(f) = \int x(t) e^{-j2\pi tf} dt \tag{6}$$

is Fourier spectrum of input signal.

The presence of $\Phi(kf_s)$ in Eq.5 is similar to low-pass filter performance, which 3dB transmission bandwidth can be described as

$$\mathbf{BW}_{\mathtt{3dB}} \approx \frac{\kappa}{\tau_s}, \tag{7}$$

where τ_s aperture time defined on full width on half maximum (FWHM), κ is time-bandwidth product, that is $\sim$0.315 for $\mathbf{sech}^2$ pulses and $\sim$0.44 for Gaussian pulses.

Typical pulse width of commercially available gigahertz rate MLLs is in the range of 250–1000 fs, so the input bandwidth of one channel PhADC (Fig.1), can be as high as 1–4 THz, that is higher than that for off-the-shelve EOMs and PDs, which typical bandwidth does not exceed 100 GHz. So, this scheme is limited by the parameters of electrooptic and optoelectronic components, not by the optical paths. For the pulsed light sources with 10 fs jitter it is possible to downconvert an digitize signals from 100 GHz band with up to 8 ENOB precision using the scheme from Fig.1 built on available components.

Preprints (www.preprints.org) | NOT PEER-REVIEWED | Posted: 14 November 2022 doi:10.20944/preprints202211.0229.v1

In the case of multichannel PhADC with PC-module based on optical fiber group velocity dispersion (GVD) effect causes elongation of aperture time. For N channel PhADC based on MLL with pulse repetition period T_{rep} the required fiber length can be estimated as

$$L_{PC} = \frac{T_{rep}}{N2\pi|\beta_2|\mathbf{ICBW}}, \tag{8}$$

where β_2 is a second order GVD coefficient of optical fiber, **ICBW** is inter-channel bandwidth. According to this an aperture time can be estimated as

$$\tau_s = 2\pi|\beta_2|\mathbf{CBW}L_{PC} = \frac{T_{rep}}{N}\frac{\mathbf{CBW}}{\mathbf{ICBW}}, \tag{9}$$

where **CBW** is DWDM module channel bandwidth, which is 100 GHz for standard ITU-DWDM module. Assuming Eq.7, it can be seen that input signal bandwidth of N-channel dispersive chirp PhADC is determined by laser parameters, number of channels and the ratio of DWDM channel bandwidth to inter-channel bandwidth.

3. Methods

The numeric modeling of ultra-short laser pulses propagation through optical fiber is typically performed using the decision of nonlinear Schrödinger equation in the form [18]:

$$\frac{\partial a}{\partial z} + \frac{\alpha}{2}a + \frac{j}{2}\beta_2\frac{\partial^2 a}{\partial T^2} = j\gamma|a|^2 a \tag{10}$$

where $T = t - z/v_g = t - z\beta_1$ (v_g — group velocity) is time variable within temporal window that shifts with pulse along fiber; $a(z,T)$ is a pulse amplitude envelop complex function; α is attenuation coefficient; β_2 is 2-nd order GVD coefficient; $\gamma = n_2\omega_0/cA_{eff}$ is nonlinear parameter, where A_{eff} effective mode cross-section.

Equation 10 can be solved using the algorithmic implementation of fourth-order Runge-Kutta method in the interaction picture method (RK4IP) [19–21]. Figure 3 demonstrates the results of numeric and experimental investigation of 250 fs pulses propagation through single-mode fiber with 1 km length. We used the next parameters of fiber in the model taken from handbook data: β_2 = -25.37 ps^2/km, γ = 1.19 rad/W·km. In the case of experimental modeling pulsed train from MLL was sent to fiber patch cord, detected using 40 GHz bandwidth photo-detector and analyzed using oscilloscope with 33 GHz input bandwidth. It can be seen that the numeric result correspond to the result obtained in experiment.

Preprints (www.preprints.org) | NOT PEER-REVIEWED | Posted: 14 November 2022 doi:10.20944/preprints202211.0229.v1

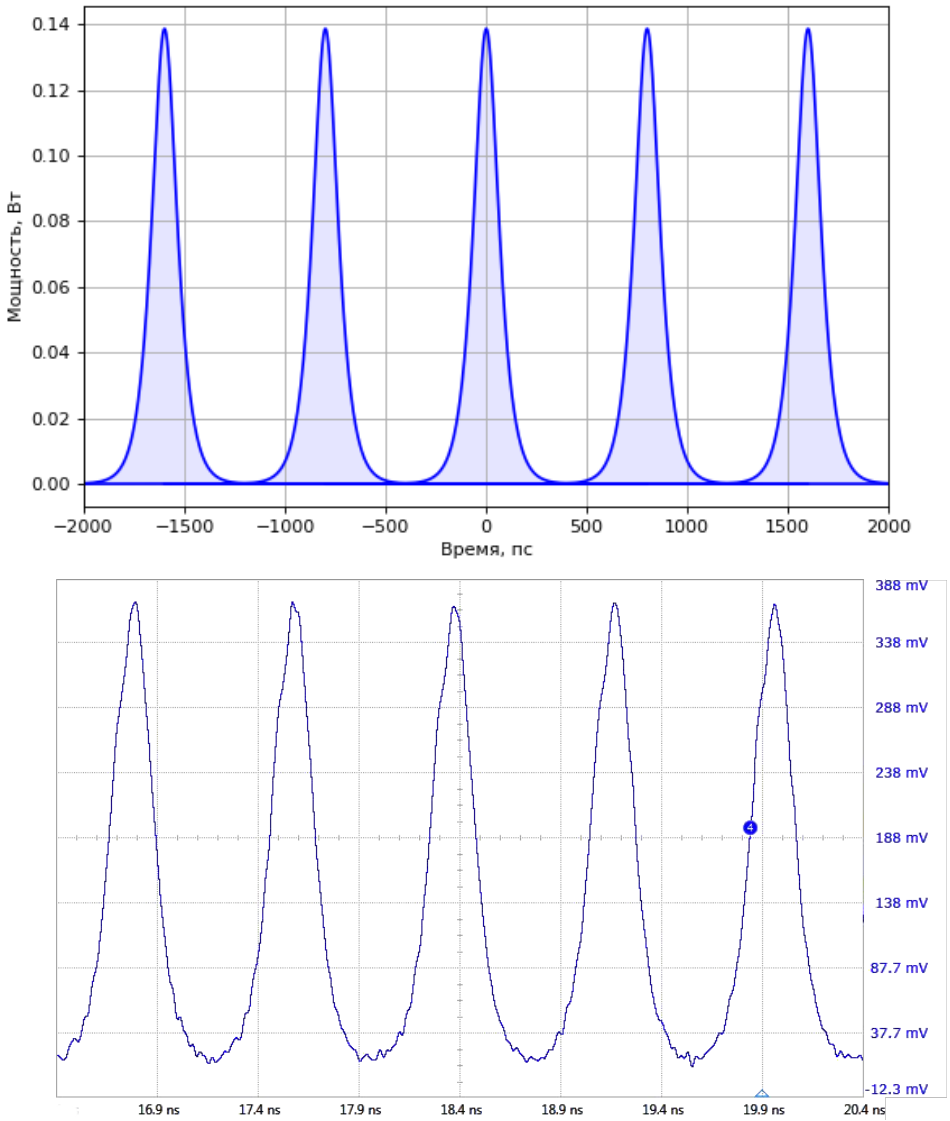

Figure 3. The results of numeric (top) and experimental (bottom) investigations of 250 fs ultra-short laser pulses train propagation through optical fiber line with the length of 1 km.

4. Modeling results

Table 1 and Fig.4 demonstrate the parameters and modeling results for different DWDM channels configurations of 4-channel dispersive time stretch module and for **sech**^{2}-formed initial pulses.

Table 1. Parameters of simulated models

Parameter	Units	Value			
ICBW	GHz	100	200	300	400
L,	km	12.68	6.34	4.23	3.1
T_G,	ps	200	100	75	50
BW$_{3dB}$,	Ghz	1.88	3.75	5.63	7.25

The modeling results demonstrate, that the less bandwidth between DWDM channels used in the scheme the longer fiber length is required to perform the desired chirp of initial light pulses in order to obtain equidistant distribution of spectral components within the

Preprints (www.preprints.org) | NOT PEER-REVIEWED | Posted: 14 November 2022 doi:10.20944/preprints202211.0229.v1

H

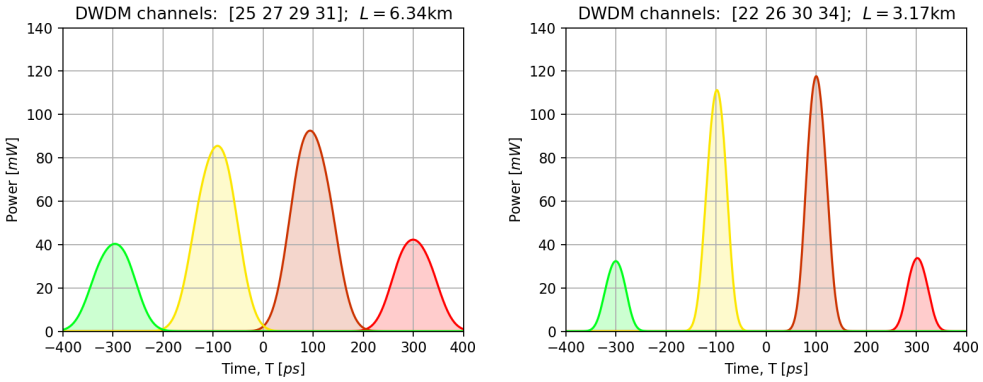

Figure 4. Numeric simulation of 4-channel continuous chirp system output signal for different cases of DWDM channels selection mean power $f_{rep} = 1.25$ GHz, $P_m = 100$ mW, $E_0 = 80$ pJ: **(a)** fiber length L=6.34 km, numbers of channels 25,27,29,31 ; **(b)** fiber length L=3.17.34 km, numbers of channels 22,26,30,34.

repetition period. In the case of adjacent channels more than 12 km of optical fiber is required to maintain the desired chirp. Dispersion of the fiber causes temporal broadening of the spectral components up to 200 ps that limits input signal frequency range to only 15.8 GHz for $\mathbf{sech}^2$ pulses. Selection of non adjacent channels allows to shorten the length of fiber proportionally to inter channel bandwidth increase and obtain up to about 70 GHz in the case of 400 GHz difference between channels. However, it must be noted that strong diversity of mean power within the spectral channels is obtained in the last case. Also the mean power of outer channels is less than 1 mW that is not enough for detection with high dynamic range.

A straightforward decision of low power outer channels problem is the use of optical amplifiers in these channels. Undesired consequence in this case is added noise and complication of overall scheme. The use of light source with higher output power can increase the power of outer channels. However the effect of self-phase modulation (SPM) must be considered during the development of dispersive time-stretch PhADC on the base of long fiber line. Propagation of high energy pulses through optical fiber results in deformation of pulses envelop and redistribution of energy within its optical spectrum amplifying the components close to central wavelength. Also, combination of anomalous dispersion of optical fiber in 1.5 mkm spectral region with SPM results in satisfaction of soliton formation conditions that cause a drastic distortion of sampling sequence. Figure 5 demonstrates the modeling results of 4-channel sampling sequence for different values of pulse energy. It can be seen that increase of pulse energy P_0 above 87 pJ results in formation of soliton at the center of time window.

5. Discussion

Modeling results demonstrate the main limitations of optical sampling multichannel PhADC on the base of ultra-short laser pulses dispersive chirp using optical fiber. Modeling algorithms, which are based on nonlinear Schrödinger equation decision using well confirmed methods, showed that intrinsic fiber effects such as dispersion and self phase modulation cause limitations of input signal bandwidth and sampling source power correspondingly. For pulsed light source based on mode-locked laser with central wavelength of 1555 nm, pulse width of 250 fs and pulse repetition rate of 1.25 GHz up to 12 channels of standard telecommunication 100 GHz ITU DWDM module can be used in the scheme providing the possibility to increase the sampling rate up to 12 times. Depending on the source pulse repetition rate, multiplication rate and selected DWDM channels input signal

Preprints (www.preprints.org) | NOT PEER-REVIEWED | Posted: 14 November 2022 doi:10.20944/preprints202211.0229.v1

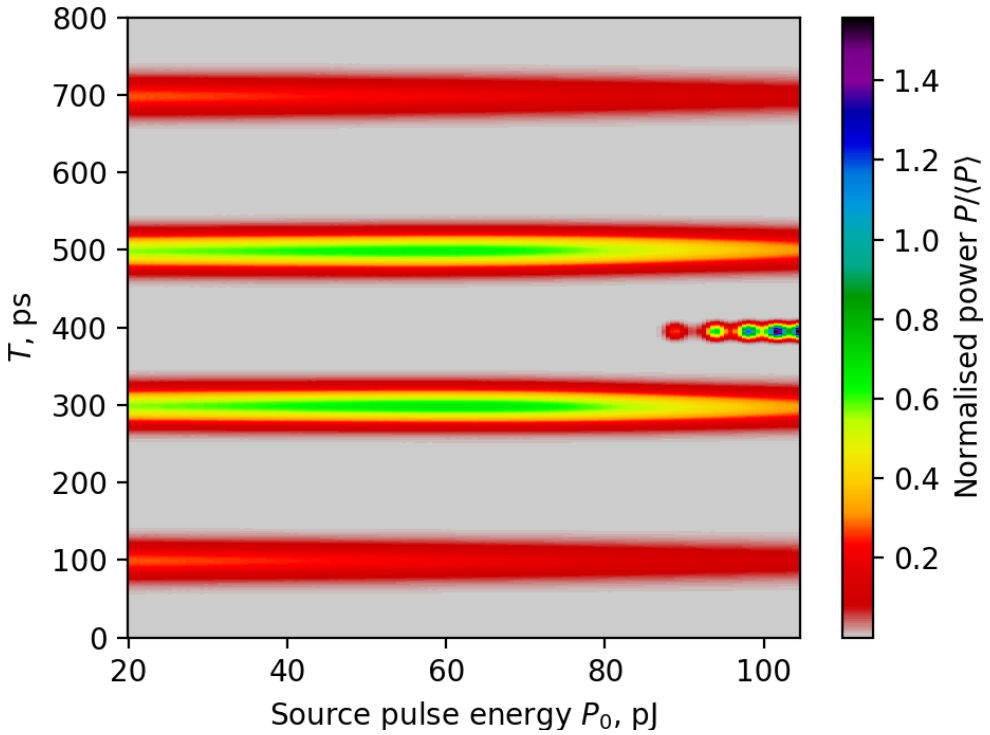

Figure 5. The dependence of normalized power distribution within repetition period of MLL pulses train for 4-channel continuous chirp PhADC from source pulse energy: $L = 3.17$ km, $f_{rep} = 1.25$ GHz, $N = 4$, $\lambda_0 = 1555$ nm, $\beta_2 = -25.37$ ps^2/km, $\gamma = 1.19$ rad/W·km.

bandwidth is limited due to strong dispersion effect of optical fiber that causes elongation of sampling pulses and increase of aperture time. For 1.25 GHz of MLL repetition rate the maximum of input bandwidth of 7.25 GHz can be obtained in the scheme using standard telecommunication equipment. According to Eq.9 the use of 2.5 GHz MLL source and 50 GHz DWDM technology allows to obtain 4x increase of input signal bandwidth and reach up to 29 GHz. The maximum of input bandwidth can be reached when outermost DWDM channels within laser spectrum together with channels close to central wavelength are used in the scheme. It leads to strong power difference between channels and very low power in outer channels. We obtained that for typical MLL with 1.25 GHz of pulse repetition rate and 50 mW of mean power (40 pJ of source pulse energy) the output mean power in outer channels is less than 1 mW that is not enough for high linear detection. Increase of MLL output power can be possible decision of this problem, however rise of pulses energy above 87 pJ threshold causes formation of soliton due to combined effect of self phase modulation and anomalous dispersion.

Author Contributions: Conceptualization E.Z.,R.S.; writing—original, draft preparation V.N., E.Z.; editing V.N. All authors have read and agreed to the published version of the manuscript.

Funding: This work was supported by ”Priority 2030”

Conflicts of Interest: The authors declare no conflict of interest.

Abbreviations

The following abbreviations are used in this manuscript:

 doi:10.20944/preprints202211.0229.v1

PhADC	Photonic analogue to digital converter
EOM	Electro-optical modulator
PD	Photodetector
EQ	Electronic quantizer
DM	Denultiplexer

References

1. Valley, G.C. Photonic analog-to-digital converters. *Optics Express* **2007**, *15*, 1955–1982. https://doi.org/10.1364/OE.15.001955.
2. Pierno, L.; Dispenza, M.; Tonelli, G.; Bogoni, A.; Ghelfi, P.; Poti, L. A photonic ADC for radar and EW applications based on modelocked laser. In Proceedings of the 2008 International Topical Meeting on Microwave Photonics jointly held with the 2008 Asia-Pacific Microwave Photonics Conference, 2008, pp. 236–239. https://doi.org/10.1109/MWP.2008.4666680.
3. Khilo, A.; Spector, S.J.; Grein, M.E.; Nejadmalayeri, A.H.; Holzwarth, C.W.; Sander, M.Y.; Dahlem, M.S.; Peng, M.Y.; Geis, M.W.; DiLello, N.A.; et al. Photonic ADC: overcoming the bottleneck of electronic jitter. *Optics Express* **2012**, *20*, 4454–4469. https://doi.org/10.1364/OE.20.004454.
4. Ng, W.; Rockwood, T.D.; Sefler, G.A.; Valley, G.C. Demonstration of a Large Stretch-Ratio (M = 41) Photonic Analog-to-Digital Converter With 8 ENOB for an Input Signal Bandwidth of 10 GHz. *IEEE Photonics Technology Letters* **2012**, *24*, 1185–1187. https://doi.org/10.1109/LPT.2012.2198881.
5. Esman, D.J.; Wiberg, A.O.J.; Yang, M.H.; Liu, L.; Kuo, B.P.P.; Alic, N.; Radic, S. Photonic parametric sampled analog-to-digital conversion at 100 GHz and 6 ENOBs. In Proceedings of the 2014 The European Conference on Optical Communication (ECOC), 2014, pp. 1–3. https://doi.org/10.1109/ECOC.2014.6964086.
6. Starikov, R.S. Photonic sampled ADC's: State of the art. International Society for Optics and Photonics, 2017, Vol. 10176. https://doi.org/10.1117/12.2268144.
7. Benedick, A.J.; Fujimoto, J.G.; Kärtner, F.X. Optical flywheels with attosecond jitter. *Nature Photonics* **2010**, *6*, 97–100. https://doi.org/10.1038/nphoton.2011.326.
8. Kim, H.; Qin, P.; Song, Y.; Yang, H.; Shin, J.; Kim, C.; Jung, K.; Wang, C.; Kim, J. Sub-20-Attosecond Timing Jitter Mode-Locked Fiber Lasers. *IEEE Journal of Selected Topics in Quantum Electronics* **2014**, *20*, 0901108. https://doi.org/10.1109/JSTQE.2014.2298454.
9. Hirschman, J.; Lemons, R.; Chansky, E.; Steinmeyer, G.; Carbajo, S. Long-term Hybrid Stabilization of the Carrier-Envelope Phase. *Optics Express* **2020**, *28*, 34093–34103. https://doi.org/10.1364/OE.400321.
10. Emaury, F.; Rudin, B. Space-grade fs mode-locked laser at 2.5 GHz and 1550 nm: results and applications. In Proceedings of the Frontiers in Ultrafast Optics: Biomedical, Scientific, and Industrial Applications XXII. International Society for Optics and Photonics, SPIE, 2022, Vol. PC11991. https://doi.org/10.1117/12.2610198.
11. Treacy, E. Optical pulse compression with diffraction gratings. *IEEE Journal of Quantum Electronics* **1969**, *5*, 454–458. https://doi.org/10.1109/JQE.1969.1076303.
12. Martinez, O. 3000 times grating compressor with positive group velocity dispersion: Application to fiber compensation in 1.3-1.6 μm region. *IEEE Journal of Quantum Electronics* **1987**, *23*, 59–64. https://doi.org/10.1109/JQE.1987.1073201.
13. Martinez, O.E.; Gordon, J.P.; Fork, R.L. Negative group-velocity dispersion using refraction. *Journal of the Optical Society of America A* **1984**, *1*, 1003–1006. https://doi.org/10.1364/JOSAA.1.001003.
14. Yariv, A.; Koumans, R. Time interleaved optical sampling for ultra-high speed A/D conversion. *Electronics Letters* **1998**, *34*, 2012–2013(1). https://doi.org/10.1049/el:19981428.
15. Kang, J.; Esman, R. Demonstration of time interweaved photonic four-channel WDM sampler for hybrid analogue-digital converter. *Electronics Letters* **1999**, *35*, 60–61(1). https://doi.org/10.1049/el:19990041.
16. Frankel, M.; Kang, J.; Esman, R. High-performance photonic analogue-digital converter. *Electronics Letters* **1997**, *33*, 2096–2097. https://doi.org/10.1364/OFC.2001.WV1.
17. Fard, A.M.; Gupta, S.; Jalali, B. Photonic time-stretch digitizer and its extension to real-time spectroscopy and imaging. *Laser & Photonics Reviews* **2013**, *7*, 207–263. https://doi.org/https://doi.org/10.1002/lpor.201200015.
18. Agrawal, G. *Nonlinear Fiber Optics (Fifth Edition)*; Optics and Photonics, Academic Press: Boston, 2013.
19. Hult, J. A Fourth-Order Runge–Kutta in the Interaction Picture Method for Simulating Supercontinuum Generation in Optical Fibers. *Journal of Lightwave Technology* **2007**, *25*, 3770–3775. https://doi.org/10.1109/JLT.2007.909373.
20. Heidt, A.M. Efficient Adaptive Step Size Method for the Simulation of Supercontinuum Generation in Optical Fibers. *Journal of Lightwave Technology* **2009**, *27*, 3984–3991. https://doi.org/10.1109/JLT.2009.2021538.
21. Balac, S.; Fernandez, A.; Mahé, F.; Méhats, F.; Texier-Picard, R. The Interaction Picture method for solving the generalized nonlinear Schr odinger equation in optics. *ESAIM: Mathematical Modelling and Numerical Analysis, EDP Sciences* **2016**, *50*, 945–964. https://doi.org/10.1051/m2an/2015060.